Bull. Health Sci. Hirosaki 4 : 83—91, 2005

Quasi-monochromatic fine polycapillary imaging utilizing computed radiography system

—— X-ray lens for biomedicine ——

Toshio ICHIMARU[*1], Eiichi SATO[*2], Etsuro TANAKA[*3]
Hidezo MORI[*4], Toshiaki KAWAI[*5], Sigehiro SATO[*6]
and Kazuyoshi TAKAYAMA[*7]

(Received October 31, 2004 ; Accepted January 13, 2005)

Abstract : A fundamental study on quasi-monochromatic radiography using a polycapillary plate and a copper-target x-ray tube is described. The tube voltage was regulated from 12 to 22 kV, and the tube current was regulated within 3.0 mA by the filament temperature. The exposure time was controlled in order to obtain optimum x-ray intensity, and the maximum focal spot dimensions were approximately 2.0 × 1.5 mm. The polycapillary plate was J5022-16 (Hamamatsu Photonics Inc.), and the plate thickness was 1.0 mm. The outer, effective, and hole diameters were 33 mm, 27 mm, and 10 μm, respectively. Quasi-monochromatic x rays were produced using a 10-μm-thick copper filter with a tube voltage of 17 kV, and these rays were formed into quasi-parallel beams by the polycapillary. The radiogram was taken using a computed radiography system utilizing imaging plates. The spatial resolution hardly varied according to increases in the distance between the spatial resolution-test chart and imaging plate using a polycapillary. We could observe a 50 μm tungsten wire, and fine blood vessels of approximately 100 μm were visible in angiography.

Key words : quasi-parallel radiography, quasi-monochromatic xrays, characteristic xrays, x-ray lens, polycapillary plate

1. INTRODUCTION

Monochromatic parallel x-ray beams are typically produced by a synchrotron in conjunction with single crystals and have been applied in high contrast micro-angiography[1] and x-ray phase imaging.[2-4] In order to produce quasi-monochromatic x rays without using the synchrotron, we developed a transmission type molybdenum x-ray tube.[5] Subsequently, flash x-ray tubes are employed to

*1 Department of Radiological Technology, School of Health Sciences, Hirosaki University, 66-1 Hon-cho, Hirosaki-shi, Aomori-ken 036-8564, Japan.
E-mail: ichimaru@cc.hirosaki-u.ac.jp
*2 Department of Physics, Iwate Medical University, 3-16-1 Hon-cho-dori, Morioka-shi, Iwate-ken 020-0015, Japan.
*3 Department of Nutritional Science, Faculty of Applied Bio-science, Tokyo University of Agriculture, 1-1-1 Sakuragaoka, Setagaya-ku, Tokyo 156-8502, Japan.
*4 Department of Cardiac Physiology, National Cardiovascular Center Research Institute, 5-7-1 Fujishiro-dai, Suita-shi, Osaka 565-8565, Japan.
*5 Electron Tube Division, Hamamatsu Photonics K. K., 314-5 Shimokan-zo, Toyooka village, Iwata-gun, Shizuoka-ken, 438-0193, Japan.
*6 Department of Microbiology, School of Medicine, Iwate Medical University, 19-1 Uchimaru, Morioka-shi, Iwate-ken 020-8505, Japan.
*7 Shock Wave Research Center, Institute of Fluid Science, Tohoku University, 2-1-1 Katahira, Aoba-ku, Sendai-shi, Miyagi-ken 980-8577, Japan.

primarily perform high-speed radiographies with biomedical applications. In particular, plasma flash x-ray tubes are very useful to produce intense and sharp characteristic xrays[6-11] such as lasers.

With recent advances in x-ray optics, several different x-ray lenses[12,13] have been developed, and a polycapillary plate[5,8,14] has been shown to be useful to realize a low-priced x-ray system and to perform quasi-parallel radiography. Therefore, we performed polycapillary imaging using a tungsten-target x-ray tube and an x-ray film because the film is conventional and is useful to obtain a high image resolution.

In biomedical radiography, because both the brightness and the contrast of radiograms can be controlled by a Computed Radiography (CR) system[15] utilizing imaging plates, the CR system is useful to perform quasi-monochromatic polycapillary imaging, regardless of whether the image resolution falls.

In this article, we describe a quasi-monochromatic parallel radiography system utilizing a fine polycapillary plate with a hole diameter of 10 μm, a CR system, and a copper-target radiation tube in order to create a conventional x-ray system to be used instead of the synchrotron.

2. EXPERIMENTAL SETUP

Figure 1 shows the circuit diagram of the x-ray generator, which consists of a negative high-voltage power supply, a filament (hot cathode) power supply, and a copper-target x-ray tube. The negative high-voltage is applied to the cathode electrode, and the anode (target) is connected to the ground. In this experiment, the tube voltage was regulated from 12 to 22 kV, and the tube current was regulated by the filament temperature and ranged from 1.0 to 3.0 mA. The exposure time was controlled in order to obtain optimum x-ray intensity.

The experimental setup for performing quasi-parallel radiography is shown in Fig. 2. Quasi-monochromatic x rays are produced using a 10-μm-thick copper filter, and these rays are formed into quasi-parallel beams by a polycapillary plate (Fig. 3). The polycapillary is J5022-16 (Hamamatsu Photonics Inc.), and the thickness and the hole diameter of the polycapillary are 1.0 mm and 10 μm, respectively. Radiography

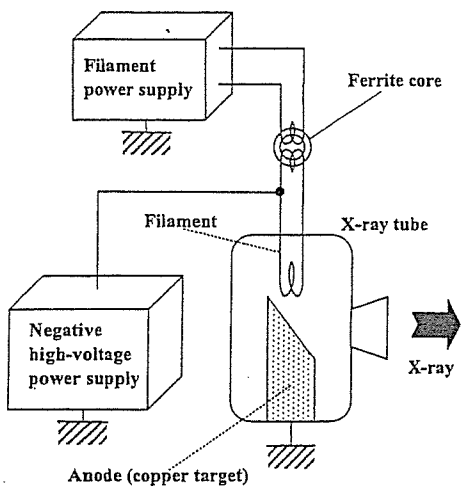

Fig. 1. Circuit diagram of the x-ray generator.

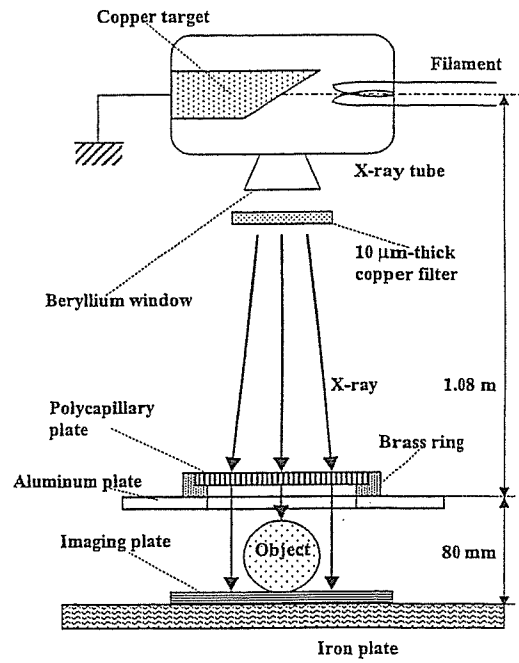

Fig. 2. Experimental setup for quasi-parallel radiography utilizing a polycapillary plate and a CR system.

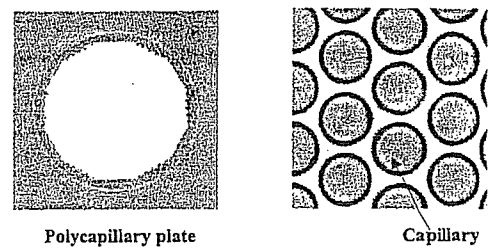

Fig. 3. Polycapillary plate.

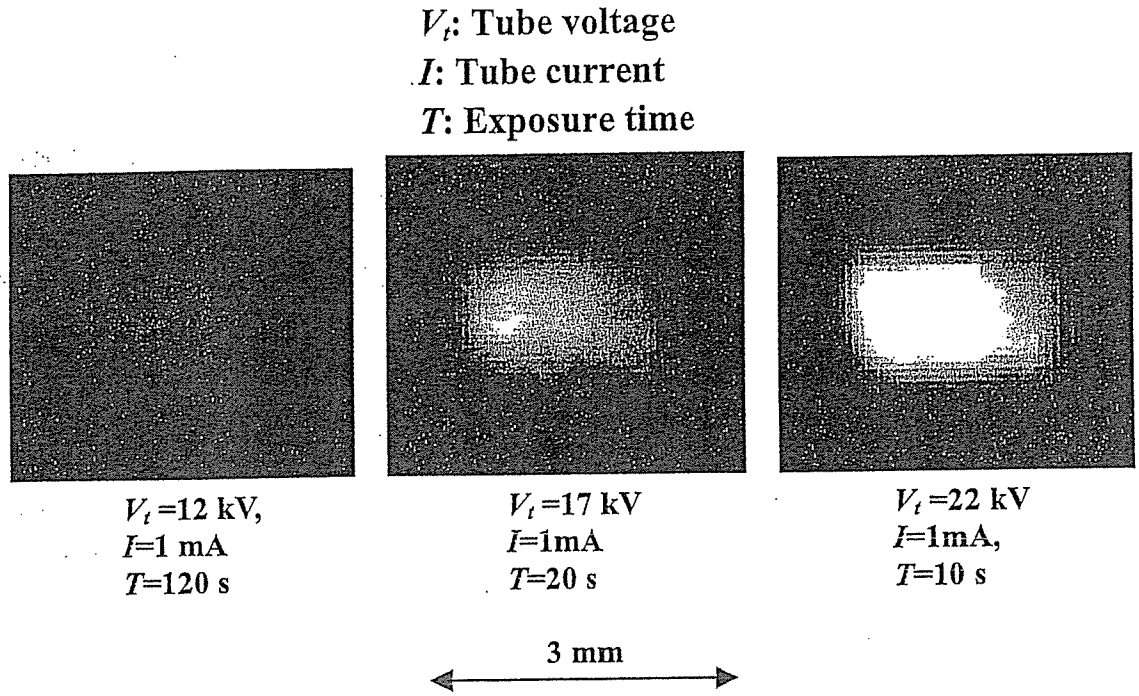

Fig. 4. Images of the x-ray source measured by a 50-μm-diameter pinhole with changes in the tube voltage.

was performed by a CR system (Konica Regius 150) utilizing imaging plates, and the distance between the x-ray source and the polycapillary was 1.08 m.

3. CHARACTERISTICS

3.1 *Focal Spot*

In order to measure images of the x-ray source, we employed a pinhole camera with a hole diameter of 50 μm (Fig. 4). When the tube voltage was increased, the spot intensity increased, and spot dimensions increased slightly and had values of approximately 2.0 × 1.5 mm.

3.2 *X-ray Spectra*

X-ray spectra from the copper-target tube were measured by a transmission-type spectrometer with a lithium fluoride curved crystal 0.5 mm in thickness. The spectra were taken by the CR system with a wide dynamic range, and relative x-ray intensity was calculated from DICOM (Digital Imaging and Communications in Medicine) digital data. Figure 5 shows measured spectra from the copper target. When the tube voltage was increased, the bremsstrahlung x-ray intensity increased, and the characteristic x-ray intensity of Kα and Kβ lines also increased. Following insertion of the copper filter, the bremsstrahlung x

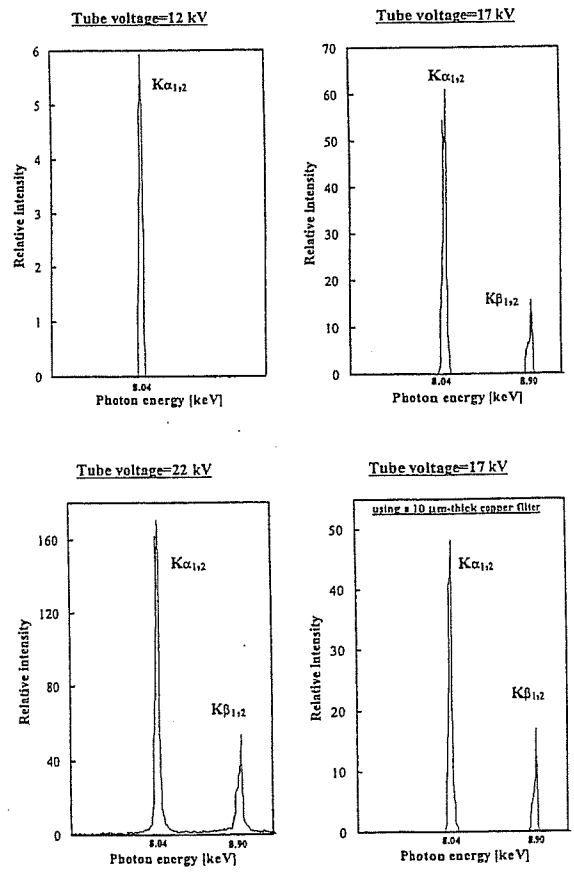

Fig. 5. Measured x-ray spectra according to changes in the tube voltage using a 10-μm-thick copper filter.

rays with energies higher than the K-absorption edge were absorbed effectively.

4. RADIOGRAPHY

The quasi-monochromatic radiography was performed with a tube voltage of 17 kV using the filter. Figure 6 shows radiography for imaging a polycapillary plate, and the radiograms of the polycapillary are shown in Fig. 7. The center of the black spot in the polycapillary radiogram was mainly imaged by direct transmission beams through capillary holes. As shown in this figure, the spot dimensions increased slightly according to decreases in the polymethyl methacrylate (PMMA) spacer height.

Figure 8 shows the polycapillary radiography for imaging a test chart, and the polycapillary was set on the brass ring. In this radiography, when the spacer height was increased, the image resolution hardly varied, and the image dimensions decreased slightly (Fig. 9). Enlarged radiograms of the test chart (166 μm lead lines) are shown in Figs. 10 and 11. When the polycapillary was employed, the image contrast of lines increased, but the resolution hardly varied. With increases in the brass spacer height, the image resolution hardly varied, and the dimensions again decreased slightly (Figs. 12 and 13). When the polycapillary was employed in conjunction with the brass spacer, the contrast again increased.

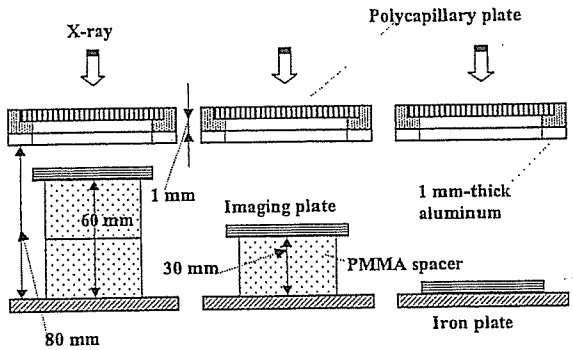

Fig. 6. Radiography for imaging a polycapillary plate according to changes in the distance between the polycapillary and imaging plates.

Figures 14 and 15 show radiography and the radiogram of tungsten wires on a PMMA spacer, respectively. Although the image contrast increased with increases in the wire diameter, a 50 μm-diameter wire could be observed. An angiography of a rabbit heart (coronary artery) is shown in Fig. 16; iodine-based microspheres of 15 μm diameter were used, and fine blood vessels of about 50 μm were visible (Fig. 17).

5. DISCUSSION

In this research, we performed quasi-parallel radiography achieved with a polycapillary plate in conjunction with quasi-monochromatic x rays, and obtained slightly higher image resolutions as compared with those obtained without using the plate.

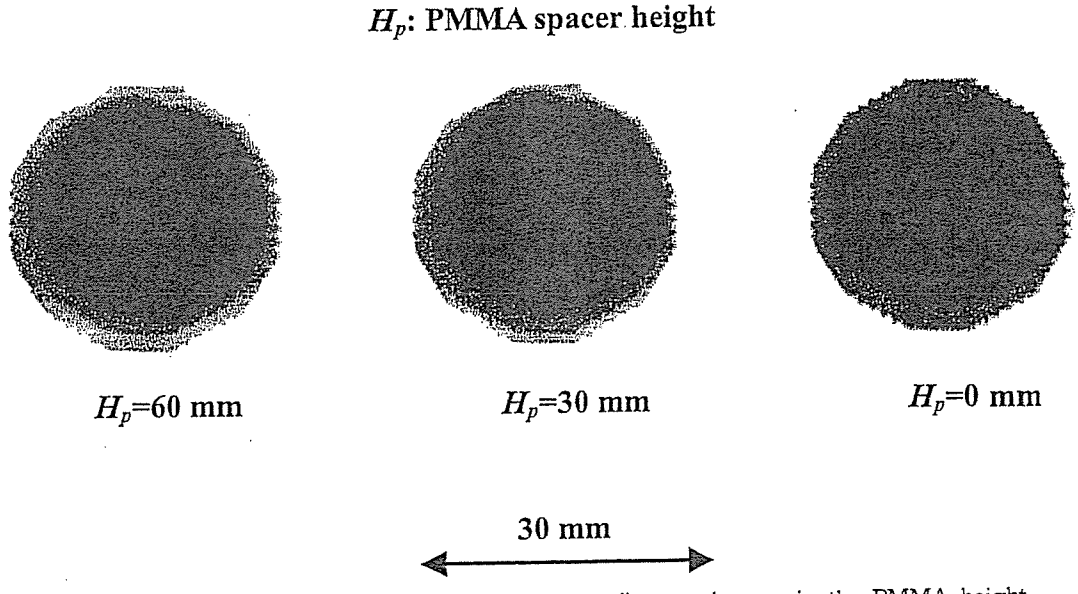

Fig. 7. Radiograms of a polycapillary plate according to changes in the PMMA height.

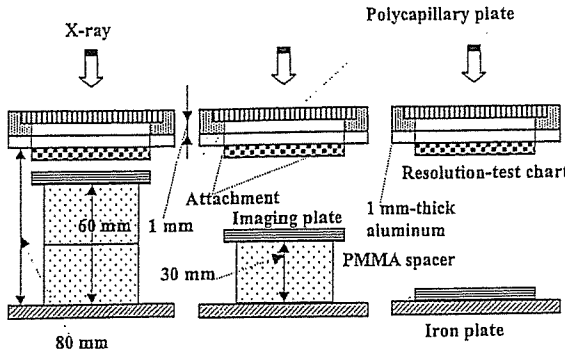

Fig. 8. Radiography for imaging a test chart using a polycapillary plate according to the PMMA height.

If we assume that the capillaries are completely straight, the image resolution of the polycapillary is primarily determined by the diameter of the capillary hole and the thickness, and is improved with decreases in the capillary diameter and increases in the thickness. In cases where the CR system is employed, although the resolution of the CR system is primarily determined by the minimum sampling pitch of 87.5 μm, we could observe 50 μm tungsten wires easily.

The photon energies of the characteristic x rays

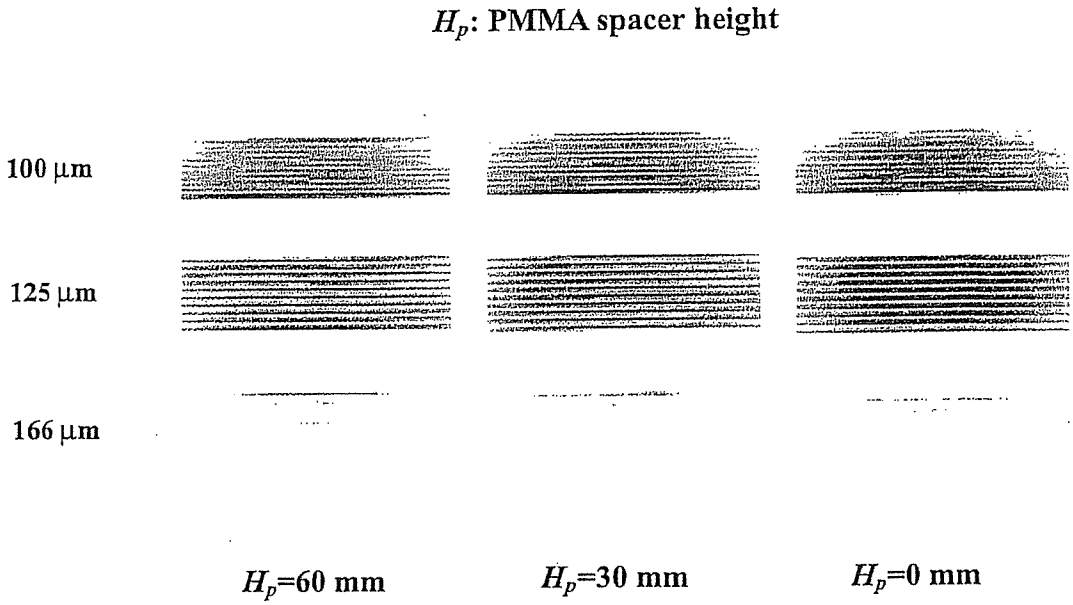

Fig. 9. Radiograms of a test chart using a polycapillary plate according to the PMMA height.

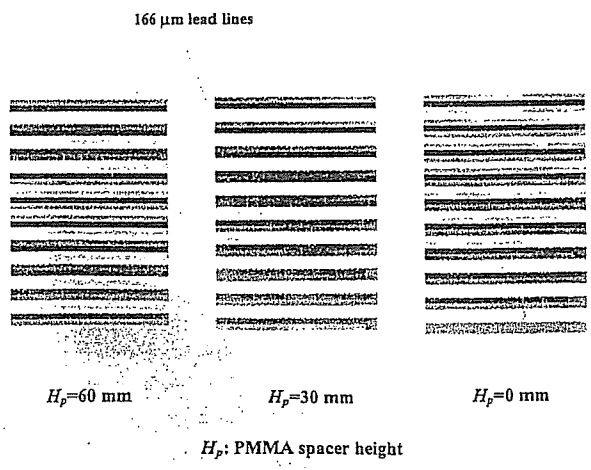

Fig. 10. Enlarged radiograms of a test chart using a polycapillary plate according to the PMMA height.

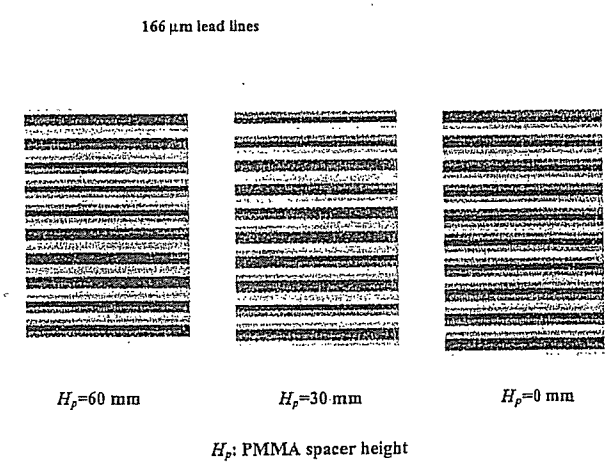

Fig. 11. Enlarged radiograms of a test chart without using a polycapillary plate according to the PMMA height.

are determined by the target element, and the capillary thickness should be increased according to increases in the photon energy because the transmission intensity through capillary glass increases. Subsequently, in order to increase the parallelity for phase imaging, single crystals should be employed after passing through the polycapillary.

Because it is possible to increase the irradiation field by increasing the distance between the x-ray source and the polycapillary, this system can be applied to image a wide variety of objects in various fields, including medical radiography.

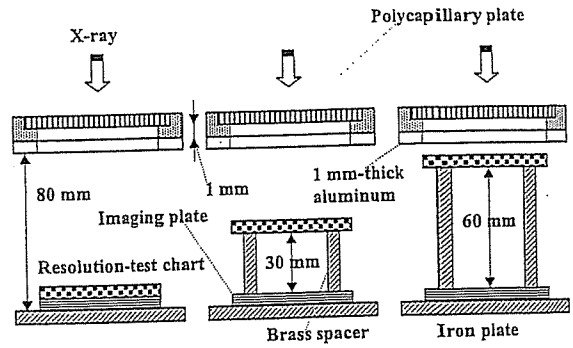

Fig. 12. Radiography for imaging a test chart using a polycapillary plate according to the brass spacer height.

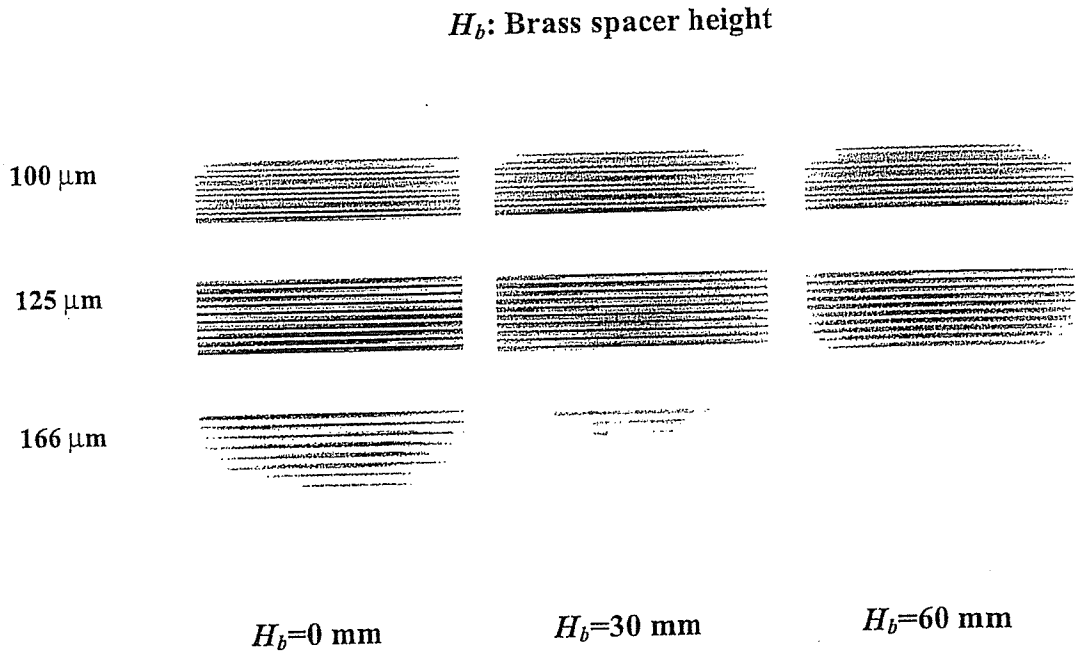

Fig. 13. Radiograms of a test chart using the polycapillary according to the brass spacer height.

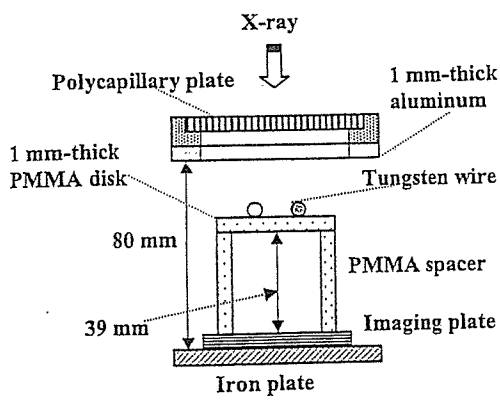

Fig. 14. Radiography for imaging tungsten wires using the polycapillary.

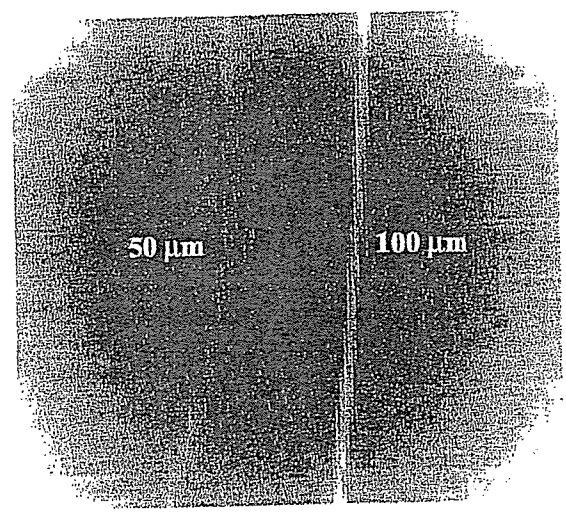

Fig. 15. Radiograms of tungsten wires on a PMMA spacer.

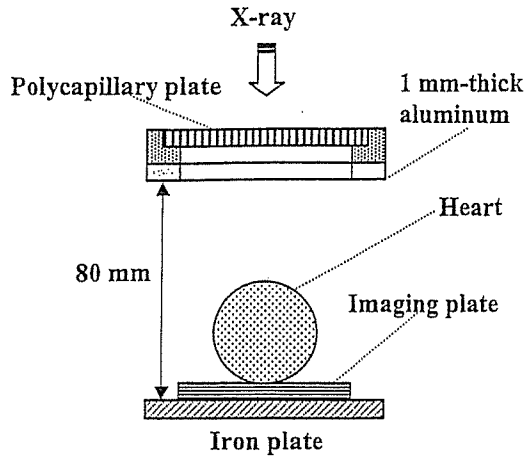

Fig. 16. Angiography of a heart extracted from a rabbit using iodine-based microspheres.

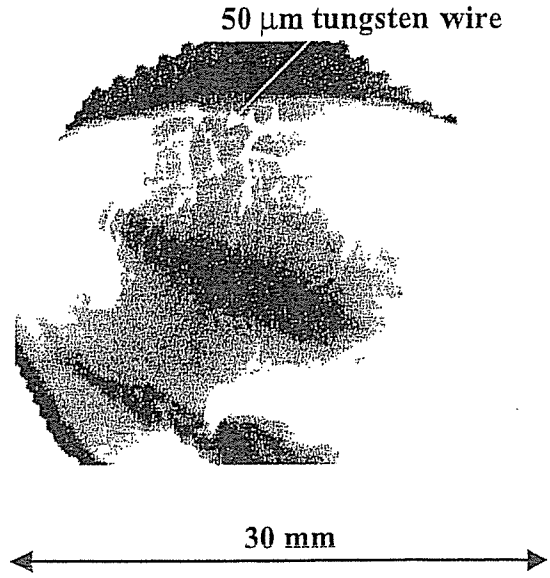

Fig. 17. Angiogram of the heart using the polycapillary.

ACKNOWLEDGMENTS

This work was supported by Grants-in-Aid for Scientific Research (13470154, 13877114, and 16591222) and Advanced Medical Scientific Research from MECSST, Health and Labor Sciences Research Grants(RAMT-nano-001, RHGTEFB-genome-005 and RHGTEFB-saisei-003), Grants from Keiryo Research Foundation, The Promotion and Mutual Aid Corporation for Private Schools of Japan, Japan Science and Technology Agency (JST), and New Energy and Industrial Technology Development Organization (NEDO, Industrial Technology Research Grant Program in '03).

REFERENCES

1) Mori H, Hyodo K, Tanaka E, Mohammed MU, Yamakawa A, Shinozaki Y, Nakazawa H, Tanaka Y, Sekka T, Iwata Y, Honda S, Umetani K, Ueki H, Yokoyama T, Tanioka K, Kubota M, Hosaka H, Ishizawa N and Ando M: Small-vessel radiography in situ with monochromatic synchrotoron radiation. *Radiology*, 201:173-177, 1996.
2) Davis TJ, Gao D, Gureyev TE, Stevenson AW and Wilkims SW: Phase-contrast imagimg of weakly absorbing materials using hard x-rays. *Nature*, 373: 595-597, 1995.
3) Momose A, Takeda T, Itai Y and Hirano K: Phase-contrast x-ray computed tomography for observing biological soft tissues. *Nature Medicine*, 2:473-475, 1996.
4) Ishisaka A, Ohara H and Honda C: A new method of analyzing edge effect in phase contrast imaging with incoherent x-rays. *Opt Rev*, 7:566-572, 2000.
5) Sato E, Komatsu M, Hayasi Y, Tanaka E, Mori H, Kawai T, Usuki T, Sato K, Ichimaru T, Takayama K and Ido H: Quasi-monochromatic parallel radiography achieved with a plane-focus x-ray tube. *Proc SPIE*, 4786:151-161, 2002.
6) Sato E, Hayasi Y, Mori H, Tanaka E, Takayama K, Ido H, Sakamaki K and Tamakawa Y: Quasi-monochromatic x-ray production from the cerium target. *Proc SPIE*, 4142:17-28, 2000.
7) Sato E, Suzuki Y, Hayasi Y, Tanaka E, Mori H, Kawai T, Takayama K, Ido H and Tamakawa Y: High-intensity quasi-monochromatic x-ray irradiation from the linear plasma target. *Proc SPIE*, 4505: 154-164, 2001.
8) Sato E, Hayasi Y, Tanaka E, Mori H, Kawai T, Obara H, Ichimaru T, Takayama K, Ido H, Usuki T, Sato K and Tamakawa Y: Polycapillary radiography using a quasi-x-ray laser generator. *Proc SPIE*, 4508:176-187, 2001.
9) Sato E, Hayasi Y, Tanaka E, Mori H, Kawai T, Usuki T, Sato K, Obara H, Ichimaru T, Takayama K, Ido H and Tamakawa Y: Quasi-monochromatic radiography using a high-intensity quasi-x-ray laser generator. *Proc SPIE*, 4682:538-548, 2002.
10) Sato E, Hayasi Y, Germer R, Tanaka E, Mori H, Kawai T, Obara H, Ichimaru T, Takayama K and Ido H: Irradiation of intense characteristic x-rays

from weakly ionized linear molybdenum plasma. *Jpn J Med Phys*, 20:123-131, 2003.

11) Sato E, Hayasi Y, Germer R, Tanaka E, Mori H, Kawai T, Obara H, Ichimaru T, Takayama K and Ido H: Intense characteristic x-ray irradiation from weakly ionized linear plasma and applications. *Jpn J Med Imag Inform Sci*, 20:148-155, 2003.

12) Xiao OF and Poturaef SV: Polycapillary-based x-ray optics. *Nucl Instr Meth Phys Res A*, 347:376-383, 1994.

13) MacDonald CA, Mail N, Li D, Roy M and Sugiro : Monochromatic applications of polycapillary optics. *Proc SPIE*, 5196:405-411, 2002.

14) Sato E, Toriyabe H, Hayasi Y, Tanaka E, Mori H, Kawai T, Usuki T, Sato K, Obara H, Ichimaru T, Takayama K, Ido H and Tamakawa Y: Fundamental study on parallel beam radiography using a polycapillary plate. *Proc SPIE*, 4682:298-310, 2002.

15) Sato E, Sato K and Tamakawa Y: Film-less computed radiography system for high-speed Imaging. *Ann Rep Iwate Med Univ Sch Lib Arts and Sci*, 35:13-23, 2000.

デジタルX線撮影システムを利用した準単色ファインポリキャピラリーイメージング
——医用X線レンズ——

市丸俊夫[*1] 佐藤英一[*2] 田中越郎[*3]
盛英三[*4] 河合敏明[*5] 佐藤成大[*6]
高山和喜[*7]

(2004年10月31日受付, 2005年1月13日受理)

要旨：ポリキャピラリープレートと銅対陰極付きX線管を用いた準単色X線撮影に関して記述した。管電圧は12から22 kVの範囲で調整され，管電流はフィラメントの温度により3.0 mA以下に調整された。X線照射時間は撮影に適正なX線強度が得られるように制御され，実効焦点サイズは2.0×1.5 mmであった。ポリキャピラリープレートは浜松ホトニクス社製のJ5022-16でプレート厚は1.0 mmであった。外径，有効径，そして孔径はそれぞれ33 mm，27 mm，10 μmであった。管電圧が17 kVの条件下で銅のK系列特性（準単色）X線は，厚さ10 μmの銅フィルターを透して出力され，これらのX線はポリキャピラリーにより準平行化された。X線像はイメージングプレート付きのデジタル撮影システム（CR）により撮影された。空間分解能はテストチャートとプレート間の距離を増しても変化しなかった。撮影では50 μmのタングステンワイヤーが認識され，造影では100 μm程度の微小血管が観察できた。

キーワード：準平行X線撮影，準単色X線，特性X線，X線レンズ，ポリキャピラリープレート

*1弘前大学医学部保健学科放射線技術科学専攻
〒036-8565 青森県弘前市本町66番地1
E-mail: ichimaru@cc.hirosaki-u.ac.jp
*2岩手医科大学教養部物理学科
〒020-0015 岩手県盛岡市本町通3-16-1
*3東京農業大学応用生物科学部栄養科学科
〒020-0015 東京都世田谷区桜ヶ丘1-1-1
*4国立循環器センター研究所心臓生理部
〒565-8565 大阪府吹田市藤白台5-7-1
*5浜松ホトニクス電子管事業部
〒438-0193 静岡県磐田郡豊岡村下神増314-5
*6岩手医科大学医学部細菌学講座
〒020-0015 岩手県盛岡市内丸19-1
*7東北大学流体力学研究所
〒980-8577 宮城県仙台市青葉区片平2-1-1

Bull. Health Sci. Hirosaki 4 : 93—100, 2005

Cone-beam K-edge angiography utilizing cerium x-ray generator in conjunction with cerium oxide filter
—— Observation of fine blood vessels ——

Toshio ICHIMARU[*1], Akira YAMADERA[*1], Eiichi SATO[*2]
Etsuro TANAKA[*3], Hidezo MORI[*4], Toshiaki KAWAI[*5]
Sigehiro SATO[*6] and Kazuyoshi TAKAYAMA[*7]

(Received October 30, 2004 ; Accepted January 13, 2005)

Abstract : The cerium x-ray generator is useful in order to perform cone-beam K-edge angiography because K-series characteristic x rays from the cerium target are absorbed effectively by iodine-based contrast mediums. The x-ray generator consists of a main controller and a unit with a high-voltage circuit and a fixed anode x-ray tube. The tube is a glass-enclosed diode with a cerium target and a 0.5 mm-thick beryllium window. The maximum tube voltage and current were 65 kV and 0.4 mA, respectively, and the focal-spot sizes were 1.2 × 0.8 mm. Cerium K-series characteristic x rays were left using a cerium oxide filter, and the x-ray intensity was 0.50 μC/kg•s at 1.0 m from the source with a tube voltage of 60 kV, a current of 0.40 mA, and an exposure time of 1.0 s. Angiography was performed with a computed radiography system using iodine-based microspheres 15 μm in diameter. In angiography of non-living animals, we observed fine blood vessels of approximately 100 μm with high contrasts.

Key words : x-ray generator, cerium target, quasi-monochromatic x rays, characteristic x rays, K-edge angiography

1. INTRODUCTION

Monochromatic parallel x-ray beams are the basis of radiography using synchrotrons in conjunction with single crystals, and these beams have been employed to perform enhanced K-edge angiography [1-3] and x-ray phase imaging.[4-6] In angiography, the beams with photon energies of approximately 35 keV are absorbed effectively by iodine-based contrast mediums. However, it is difficult to obtain sufficient machine times for various research projects, including medical applications. Subsequently, monochromatic cone beams with energies of approximately 35 keV are useful in order to increase the irradiation field

*1 Department of Radiological Technology, School of Health Sciences, Hirosaki University, 66-1 Hon-cho, Hirosaki-shi, Aomori-ken 036-8564, Japan.
*2 Department of Physics, Iwate Medical University, 3-16-1 Hon-cho-dori, Morioka-shi, Iwate-ken, 020-0015, Japan.
*3 Department of Nutritional Science, Faculty of Applied Bio-science, Tokyo University of Agriculture, 1-1-1 Sakuragaoka, Setagaya-ku, Tokyo 156-8502, Japan.
*4 Department of Cardiac Physiology, National Cardiovascular Center Research Institute, 5-7-1 Fujishiro-dai, Suita-shi, Osaka 565-8565, Japan.
*5 Electron Tube Division, Hamamatsu Photonics K. K., 314-5 Shimokan-zo,Toyooka village, Iwata-gun, Shizuoka-ken, 438-0193, Japan.
*6 Department of Microbiology, School of Medicine, Iwate Medical University, 19-1 Uchimaru, Morioka-shi, Iwate-ken 020-8505, Japan.
*7 Shock Wave Research Center, Institute of Fluid Science, Tohoku University, 2-1-1 Katahira, Aoba-ku, Sendai-shi, Miyagi-ken 980-8577, Japan.

for K-edge angiography.

In order to perform high-speed medical radiography, although several different flash x-ray generators [7-13] utilizing cold-cathode tubes have been developed, plasma flash x-ray generators[14-18] are useful to produce quasi-monochromatic x rays without using a K-edge filter. Therefore, we have performed a demonstration of cone-beam K-edge angiography[19] utilizing a cerium plasma generator, since K-series characteristic x rays from the cerium target are absorbed effectively by iodine.

Recently, we have developed a steady state x-ray generator utilizing a cerium-target tube, and have demonstrated enhanced K-edge angiography utilizing a barium sulfate filter.[20] In this research, $K\alpha$ lines (34.6 keV) were left by absorbing $K\beta$ lines (39.2 keV), and bremsstrahlung x rays with photon energies of lower than the barium K-edge (37.4 keV) were also observed. However, because cerium $K\beta$ lines are also absorbed effectively by iodine, both $K\alpha$ and $K\beta$ lines should be selected to perform angiography. In measurements of x-ray spectra, although we usually employed a cadmium tellurium detector with a photon energy resolution of 1.7 keV, the resolution should be improved as much as possible to measure the characteristic x-ray intensity.

In the present research, we measured the x-ray spectra from a cerium-target tube using a germanium detector, and performed a preliminary study on cone-beam K-edge angiography achieved with cerium characteristic x rays using a cerium oxide K-edge filter.

2. GENERATOR

Figure 1 shows the block diagram of the x-ray generator, which consists of a main controller and an x-ray tube unit with a Cockcroft-Walton circuit and a cerium-target tube. The tube voltage, the current, and the exposure time can be controlled by the controller. The main circuit for producing x rays is illustrated in Fig. 2, and employed the Cockcroft-Walton circuit in order to decrease the dimensions of the tube unit. In the x-ray tube, the negative high voltage is applied to the cathode electrode, and the anode (target) is connected to the tube unit case (ground potential) to cool the anode and the target effectively. The filament heating current is supplied by an AC power supply in the controller in conjunction with an insulation transformer. The x-ray tube is a glass-enclosed diode with a cerium target and a 0.5-mm-thick beryllium window. In this experiment, the tube voltage applied was from 45 to 65 kV, and the tube current was regulated to within 0.40 mA (maximum current) by the filament temperature. The exposure time is controlled in order to obtain optimum x-ray intensity. Quasi-monochromatic x rays are produced using a cerium oxide filter for absorbing bremsstrahlung rays.

In designing the filter, the surface density of the cerium oxide powder is important, since the x rays are absorbed effectively by the powder as compared

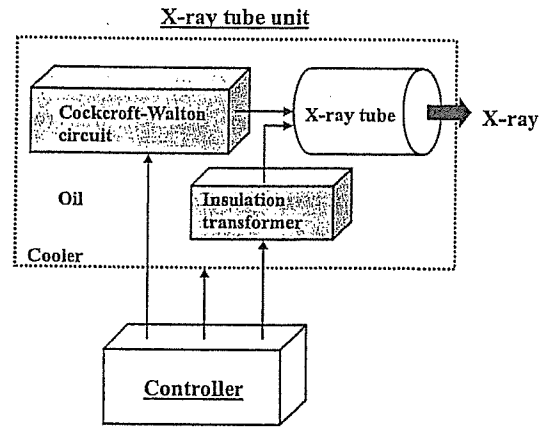

Fig. 1. Block diagram of compact x-ray generator with cerium-target radiation tube, which is used specially for K-edge angiography using iodine-based contrast mediums.

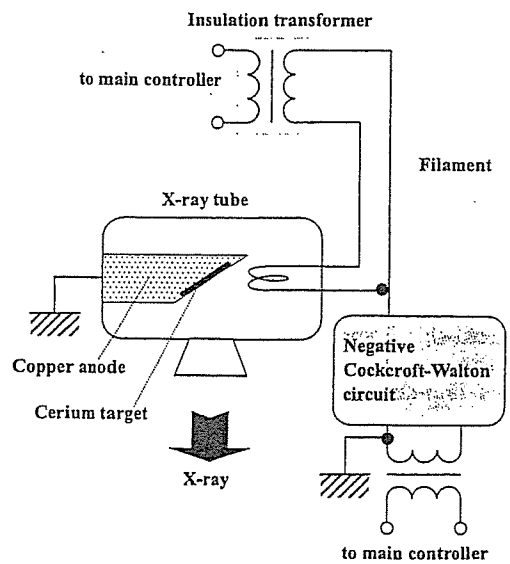

Fig. 2. Main circuit of x-ray generator.

with the PMMA powder. In this case, the density was approximately 10 mg/cm², and a K-edge powder filter (Fig. 3), consisting of cerium oxide and PMMA powders, was employed.

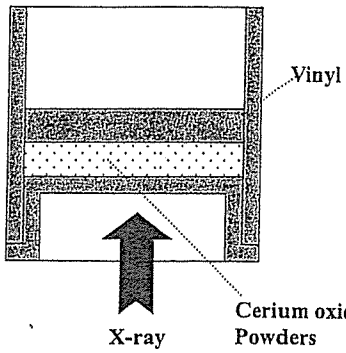

Fig. 3. Schematic drawing of cerium oxide powder filter.

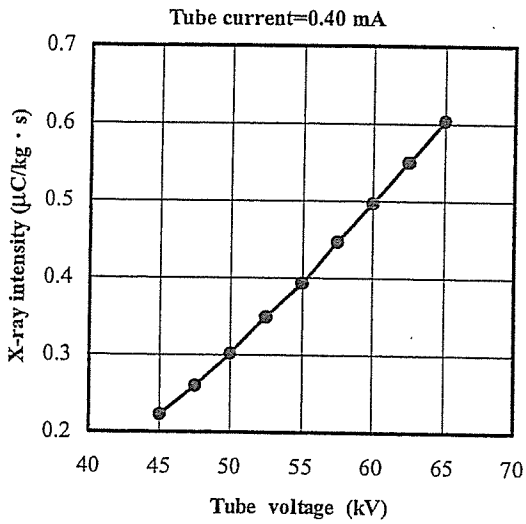

Fig. 4. X-ray intensity measured at 1.0 m from x-ray source according to changes in tube voltage.

3. CHARACTERISTICS

3.1 X-ray Intensity

X-ray intensity was measured by a Victoreen 660 ionization chamber at 1.0 m from the x-ray source using the filter (Fig. 4). At a constant tube current of 0.40 mA, the x-ray intensity increased when the tube voltage was increased. In this measurement, the intensity with a tube voltage of 60 kV and a current of 0.40 mA was 0.50 μC/kg•s at 1.0 m from the source with errors of less than 0.2%.

3.2 Focal Spot

In order to measure images of the x-ray source after the filtration, we employed a pinhole camera with a hole diameter of 50 μm (magnification ratio of 1:2) in conjunction with a Computed Radiography (CR) system[21] with a sampling pitch of 87.5 μm. When the tube voltage was increased, spot dimensions increased slightly and had values of 1.2 $\times$0.8 mm (Fig. 5).

3.3 X-ray Spectra

In order to measure x-ray spectra, we employed a germanium detector (GLP-10180/07-P, Ortec Inc.) with a photon energy resolution of approximately 0.12 keV (Fig. 6). When the tube voltage was increased, the characteristic x-ray intensities of Kα and Kβ lines substantially increased, and both the maximum photon energy and the intensities of bremsstrahlung x rays increased.

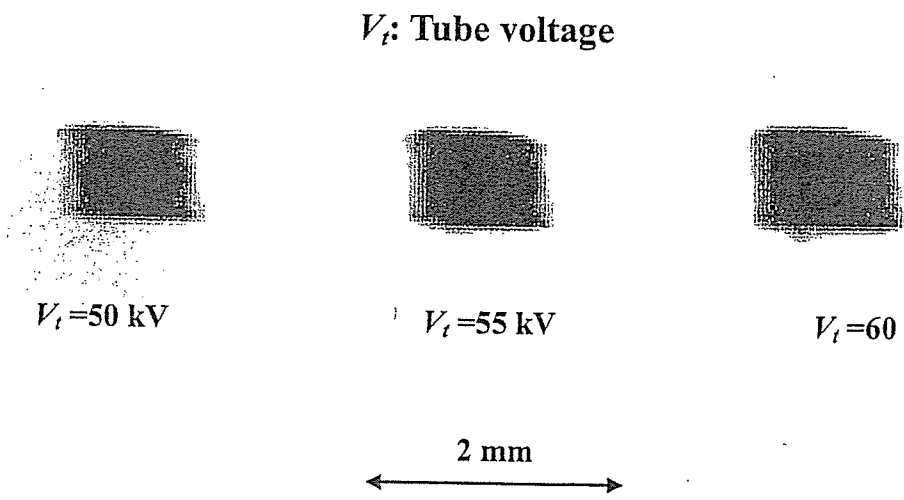

Fig. 5. Effective focal spots with changes in tube voltage.

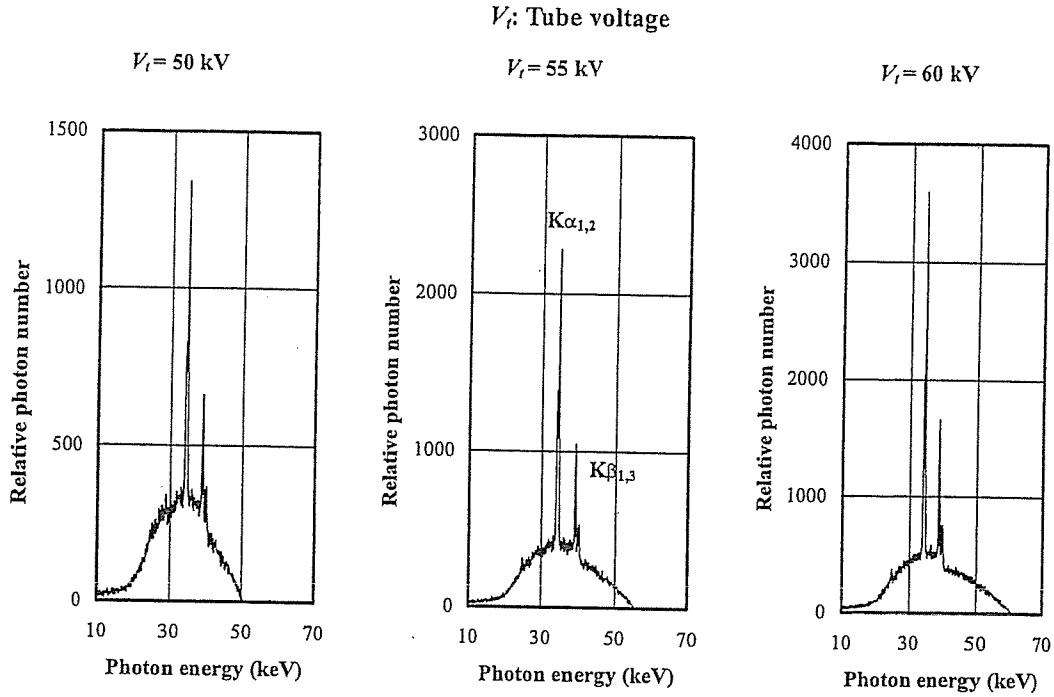

Fig. 6. X-ray spectra measured using germanium detector with changes in tube voltage.

4. K-EDGE ANGIOGRAPHY

Figure 7 shows the mass attenuation coefficients of iodine at the selected energies; the coefficient curve is discontinuous at the iodine K-edge. The average photon energy of the cerium Kα and Kβ lines are shown just above the iodine K-edge. Cerium is a rare earth element and has a high reactivity; however, the average photon energies of Kα and Kβ lines are 34.6 and 39.2 keV, respectively, and iodine contrast mediums with a K-absorption edge of 33.2 keV absorb the lines easily. Therefore, blood vessels were observed with high contrasts.

The angiography was performed by the CR system (Konica Regius 150) using the filter, and the tube voltage and the distance (between the x-ray source and the imaging plate) were 60 kV and 1.5 m, respectively. Firstly, rough measurements of spatial resolution were made using wires. Figure 8 shows radiograms of tungsten wires coiled around a rod made of polymethyl methacrylate. Although the image contrast decreased somewhat with decreases in the wire diameter, due to blurring of the image caused by the sampling pitch of 87.5 μm, a 50 μm-diameter wire could be observed.

Angiograms of rabbit hearts are shown in Fig.

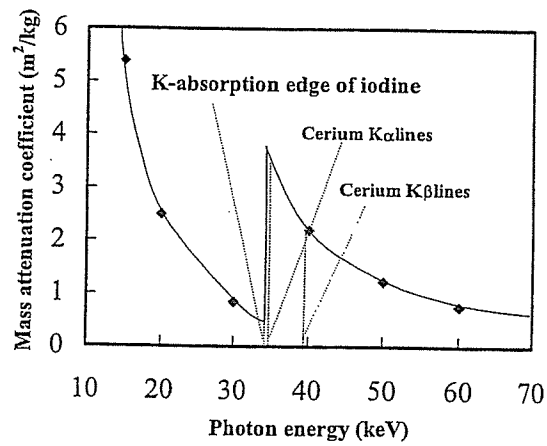

Fig.7. Mass attenuation coefficients of iodine, and average photon energies of cerium Kα and Kβ lines.

9. These two images were obtained using iodine and cerium microspheres of 15 μm in diameter. In the case where the cerium spheres were employed, the coronary arteries were barely visible. Figures 10 and 11 show angiograms of a larger dog heart and a rabbit thigh, respectively, using iodine spheres. In angiography, the coronary arteries were visible, and fine blood vessels of approximately 100 μm could be seen.

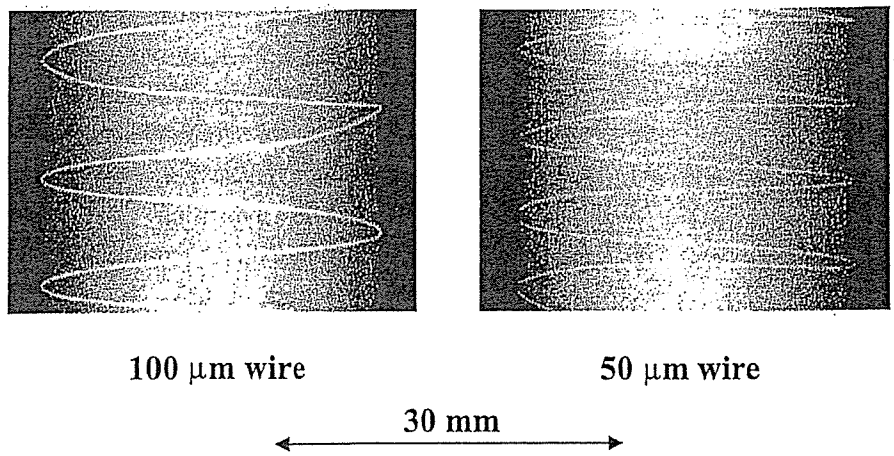

Fig. 8. Radiograms of tungsten wires in PMMA rod with tube voltage of 60 kV.

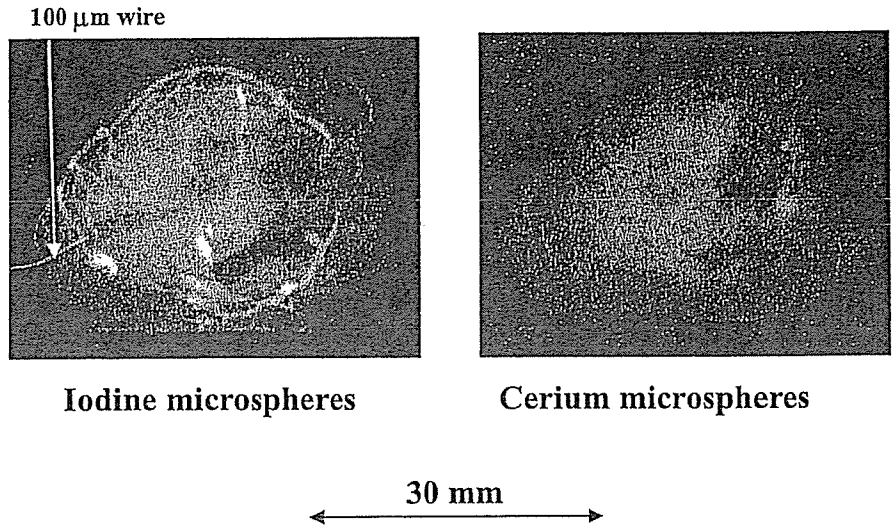

Fig. 9. Angiograms of extracted rabbit hearts using iodine and cerium microspheres with tube voltage of 60 kV.

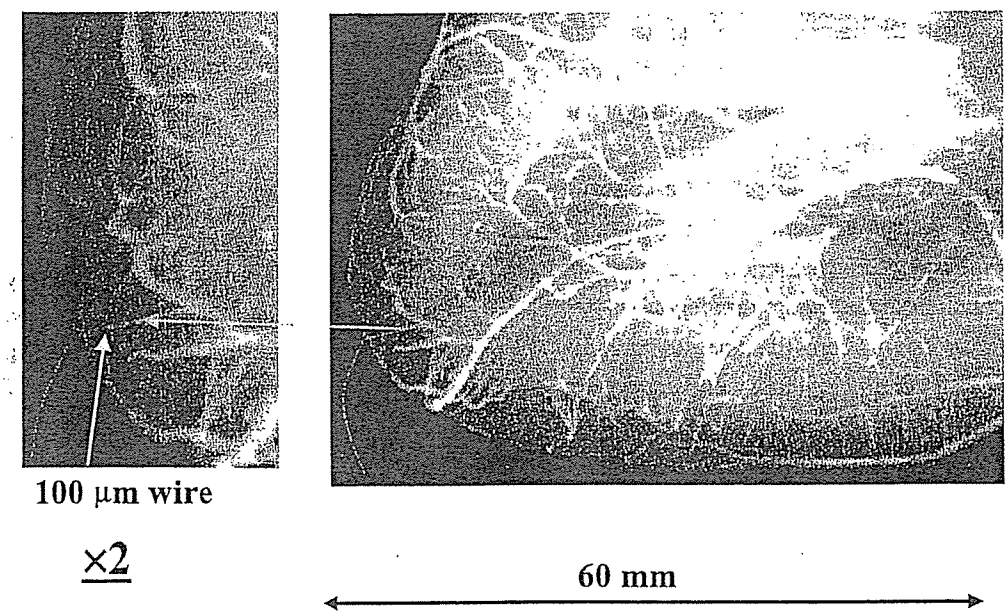

Fig. 10. Angiogram of extracted dog heart using iodine microspheres with tube voltage of 60 kV.

Fig. 11. Angiogram of rabbit thigh with tube voltage of 60 kV.

5. DISCUSSION AND CONCLUSIONS

In summary, we employed an x-ray generator with a cerium-target tube and succeeded in producing cerium characteristic x rays, which can be absorbed easily by iodine-based contrast mediums. The characteristic x-ray intensities increased with increases in the tube voltage, and bremsstrahlung rays were absorbed effectively by the filter.

Although the cerium x-ray generator used in this research produces both the characteristic and the bremsstrahlung x rays, bremsstrahlung intensity can be decreased effectively by considering the angle dependence without using the filter, since bremsstrahlung rays are not emitted in the opposite direction to that of electron acceleration. Subsequently, the generator produced maximum number of characteristic photons was approximately 3×10^7 photons/cm^2 • s at 1.0 m from the source, and the photon count rate can be increased easily by improving the target.

ACKNOWLEDGMENT

This work was supported by Grants-in-Aid for Scientific Research (13470154, 13877114, and 16591222) and Advanced Medical Scientific Research from MECSST, Health and Labor Sciences Research Grants (RAMT-nano-001, RHGTEFB-genome-005 and RHGTEFB-saisei-003), Grants from Keiryo Research Foundation, The Promotion and Mutual Aid Corporation for Private Schools of Japan, Japan Science and Technology Agency (JST), and New Energy and Industrial Technology Development Organization (NEDO, Industrial Technology Research Grant Program in '03).

REFERENCES

1) Thompson A C, Zeman H D, Brown G S, Morrison J, Reiser P, Padmanabahn V, Ong L, Green S, Giacomini J, Gordon H and Rubenstei E: First operation of the medical research facility at the NSLS for coronary angiography. *Rev. Sci. Instrum.*, 63:625-628, 1992.

2) Mori H, Hyodo K, Tanaka E, Mohammed M, Yamakawa A, Shinozaki Y, Nakazawa H, Tanaka Y, Sekka T, Iwata Y, Honda S, Umetani K, Ueki H, Yokoyama T, Tanioka K, Kubota M, Hosaka H, Ishizawa N and Ando M: Small-vessel radiography in situ with monochromatic synchrotoron radiation. *Radiology*, 201:173-177, 1996.

3) Hyodo K, Ando M, Oku Y, Yamamoto S, Takeda T, Itai Y, Ohtsuka S, Sugishita Y and Tada J: Development of a two-dimensional imaging system for clinical applications of intravenous coronary angiography using intense synchrotron radiation produced by a multipole wiggler. *J. Synchrotron Rad.*, 5:1123-1126, 1998.

4) Davis T J, Gao D, Gureyev T E, Stevenson A W and Wilkims S W: Phase-contrast imagimg of weakly absorbing materials using hard x-rays. *Nature*, 373:595-597, 1995.

5) Momose A, Takeda T, Itai Y and Hirano K: Phase-contrast x-ray computed tomography for observing biological soft tissues. *Nature Medicine*, 2:473-475, 1996.

6) Ando M, Maksimenko A, Sugiyama H, Pattanasiriwisawa W, Hyodo K and Uyama C: A simple x-ray dark- and bright- field imaging using achromatic Laue optics. *Jpn. J. Appl. Phys.*, 41: L1016-L1018, 2002.

7) Sato E, Kimura S, Kawasaki S, Isobe H, Takahashi K, Tamakawa Y and Yanagisawa T: Repetitive flash x-ray generator utilizing a simple diode with a new type of energy-selective function. *Rev. Sci. Instrum.*, 61:2343-2348, 1990.

8) Sato E, Sagae M, Takahashi K, Oizumi T, Ojima

H, Takayama K, Tamakawa Y, Yanagisawa T, Fujiwara A and Mitoya K: High-speed soft x-ray generators in biomedicine. *SPIE*, 2513:649-667, 1994.

9) Sato E, Sagae M, Takahashi K, Shikoda A, Oizumi T, Ojima H, Takayama K, Tamakawa Y, Yanagisawa T, Fujiwara A and Mitoya K: Dual energy flash x-ray generator, *SPIE*, 2513:723-735, 1994.

10) Shikoda A, Sato E, Sagae M, Oizumi T, Tamakawa Y and Yanagisawa T: Repetitive flash x-ray generator having a high-durability diode driven by a two-cable-type line pulser. *Rev. Sci. Instrum.*, 65: 850-856, 1994.

11) Sato E, Takahashi K, Sagae M, Kimura S, Oizumi T, Hayasi Y, Tamakawa Y and Yanagisawa T: Sub-kilohertz flash x-ray generator utilizing a glass-enclosed cold-cathode triode. *Med. & Biol. Eng. & Comput.*, 32:289-294, 1994.

12) Takahashi K, Sato E, Sagae M, Oizumi T, Tamakawa Y and Yanagisawa T: Fundamental study on a long-duration flash x-ray generator with a surface-discharge triode. *Jpn. J. Appl. Phys.*, 33: 4146-4151, 1994.

13) Sato E, Sagae M, Shikoda A, Takahashi K, Oizumi T, Yamamoto M, Takabe A, Sakamaki K, Hayasi Y, Ojima H, Takayama K and Tamakawa Y: High-speed soft x-ray techniques, *SPIE*, 2869: 937-955, 1996.

14) Sato E, Hayasi Y, Tanaka E, Mori H, Kawai T, Usuki T, Sato K, Obara H, Ichimaru T, Takayama K, Ido H and Tamakawa Y: Quasi-monochromatic radiography using a high-intensity quasi-x-ray laser generator. *SPIE*, 4682:538-548, 2002.

15) Sato E, Hayasi Y, Germer R, Tanaka E, Mori H, Kawai T, Obara H, Ichimaru T, Takayama K and Ido H: Intense characteristic x-ray irradiation from weakly ionized linear plasma and applications. *Jpn. J. Med. Imag. Inform. Sci.*, 20:148-155. 2003.

16) Sato E, Hayasi Y, Germer R, Tanaka E, Mori H, Kawai T, Obara H, Ichimaru T, Takayama K and Ido H: Irradiation of intense characteristic x-rays from weakly ionized linear molybdenum plasma. *Jpn. J. Med. Phys.*, 23:123-131, 2003.

17) Sato E, Hayasi Y, Germer R, Tanaka E, Mori H, Kawai T, Ichimaru T, Takayama K and Ido H: Quasi-monochromatic flash x-ray generator utilizing weakly ionized linear copper plasma. *Rev. Sci. Instrum.*, 74:5236-5240, 2003.

18) Sato E, Hayasi Y, Germer R, Tanaka E, Mori H, Kawai T, Ichimaru T, Sato S, Takayama K and Ido H: Sharp characteristic x-ray irradiation from weakly ionized linear plasma. *J. Electron Spectrosc. Related Phenom.*, 137-140:713-720, 2004.

19) Sato E, Germer R, Hayasi Y, Murakami K, Koorikawa Y, Tanaka E, Mori H, Kawai T, Ichimaru T, Obata F, Takahashi K, Sato S, Takayama K and Ido H: Weakly ionized cerium plasma radiography. *SPIE*, 5210:12-21, 2003.

20) Sato E, Tanaka E, Mori H, Kawai T, Ichimaru T, Sato S, Takayama K and Ido H: Demonstration of enhanced K-edge angiography using a cerium target x-ray generator. *Med. Phys.*, 31: 3017-3022, 2004.

21) Sato E, Sato K and Tamakawa Y: Film-less computed radiography system for high-speed Imaging. *Ann. Rep. Iwate Med. Univ. Sch. Lib. Arts and Sci.*, 35:13-23, 2000.

セリウムX線装置と酸化セリウムフィルターを利用したコーンビームKエッジ造影
―― 微小血管の観察 ――

市丸俊夫[*1] 山寺 亮[*1] 佐藤英一[*2]
田中越郎[*3] 盛 英三[*4] 河合敏明[*5]
佐藤成大[*6] 高山和喜[*7]

(2004年10月30日受付, 2005年1月13日受理)

要旨：セリウム対陰極から発生するK系列特性X線はヨウ素系造影剤に効率良く吸収されるので，コーンビームによるKエッジ造影に有用である。X線装置はメインコントローラー，そして高電圧回路とX線管のユニットなどからなる。X線管はガラス封じ込み二極管で，セリウム対陰極と0.5 mm厚のベリリウム窓を有する。管電圧と電流の最大値はそれぞれ65 kVと0.4 mAで，実効焦点サイズは1.3×0.9 mmであった。セリウムのK系列特性X線は酸化セリウムのフィルターを用いて制動X線を吸収することにより得られ，X線強度は線源から1.0 mの位置で，管電圧60 kV，そして管電流0.4 mAの条件下で，0.5 μC/kg•sであった。血管には直径15 μmのヨウ素プラスチック微小球が充填され，デジタル撮影装置（CR）で造影された。動物ファントムの造影では，100 μm程度の血管が高コントラストで観察できた。

キーワード：X線発生装置，セリウムターゲット，準単色X線，特性X線，Kエッジ造影

*1弘前大学医学部保健学科放射線技術科学専攻
〒036-8565 青森県弘前市本町66番地1
*2岩手医科大学教養部物理学科
〒020-0015 岩手県盛岡市本町通3-16-1
*3東京農業大学応用生物科学部栄養科学科
〒020-0015 東京都世田谷区桜ヶ丘1-1-1
*4国立循環器センター研究所心臓生理部
〒565-8565 大阪府吹田市藤白台5-7-1
*5浜松ホトニクス電子管事業部
〒438-0193 静岡県磐田郡豊岡村下神増314-5
*6岩手医科大学医学部細菌学講座
〒020-0015 岩手県盛岡市内丸19-1
*7東北大学流体力学研究所
〒980-8577 宮城県仙台市青葉区片平2-1-1

Flow-Independent Myocardial Ischemia Induced by Endothelin-1

An NADH Fluorescence Analysis

Soushin Inoue, MD, Shingo Hori, MD,† Takeshi Adachi, MD,‡ Koji Miyazaki, MD,* Shingo Kyotani, MD,§ Keiichi Fukuda, MD,* Hidezo Mori, MD,§ Hiroe Nakazawa, MD,¶ Naoki Aikawa, MD,† and Satoshi Ogawa, MD**

Abstract: The endothelin-1 (ET-1) is known to cause myocardial ischemia; however, whether this effect is entirely dependent on vasoconstriction is uncertain. The aim of this study was to characterize the myocardial ischemia after the intracoronary administration of endothelin-1, and compare it with that induced by coronary stenosis. In the left anterior descending coronary artery of 15 dogs, a mild inflow reduction (30%) was produced for 10 minutes using intracoronary endothelin-1 (46 ± 33 pmol/min) or coronary stenosis. The hearts were rapidly cross-sectioned at short axial plane and freeze-clamped within 120 milliseconds using a specially developed device to visualize and quantify the area of ischemia (%IA) with NADH fluorescence photography. The %IA was larger in the endothelin-1 group than in the stenosis group (66 ± 23 versus 18 ± 18, $P = 0.0005$); furthermore, the ischemia was transmural in the ET-1 group, but limited to subendocardium in the stenosis group. ET-1 increased the coronary arterial resistance especially in subepicardial region and produced smaller ischemic foci in microcirculation. The mechanism of larger ischemia produced by ET-1 might depend on pro-ischemic effects on myocytes and vasoconstriction of the coronary microcirculation, predominantly in the subepicardium in vivo.

Key Words: coronary circulation, endothelin-1, microcirculation, myocardial ischemia, NADH fluorescence, pro-ischemia

(*J Cardiovasc Pharmacol*™ 2005;46:810–816)

Endothelin-1 (ET-1) is the most potent vasoactive peptide derived from the endothelium[1] and constricts vascular smooth muscles to induce hypoperfusion.[2] The plasma ET-1 was found to be increased in patients with acute myocardial infarction and angina pectoris.[3] The pathophysiological role of ET-1 for ischemic heart disease is relevant but not fully clarified yet. Others and we have previously reported that the intracoronary administration of ET-1 induces a prominent coronary flow reduction, ST elevation, apical systolic bulge, and impaired left ventricular diastolic function in vivo.[4–6] The reduced cardiac function with ST-elevation indicated that ET-1 induces myocardial ischemia by decreasing coronary flow. However, the systolic bulge induced by ET-1 was unexpected and could not be explained by standard criteria for myocardial ischemia using a reduced flow model, which predominantly decreases the subendocardial blood flow.[4] Moreover, ET-1 receptor antagonists were shown to reduce the myocardial infarction size in ischemia/reperfusion models without any changes in regional myocardial blood flow, suggesting that intrinsic ET-1 has a flow-independent effect on myocardial ischemia in vivo.[7,8] In addition to its vasoconstrictive effect, ET-1 has direct effects on cardiac myocytes, including positive inotropic, chronotropic, and metabolic effects.[9–12] Therefore, myocardial ischemic metabolism and flow distribution should be compared in ET-1 administration and simple flow-reduction models.

The aim of this study was to clarify the characteristics of myocardial ischemia induced by the intracoronary administration of ET-1 under condition of controlled mild hypoperfusion in a canine model. The extension, distribution, and severity of myocardial ischemia induced by ET-1 were compared with those induced by an equivalent coronary flow reduction introduced by occluding the bypass circuit to the coronary artery. Because the severity and the distribution of metabolic changes in ET-1–induced myocardial ischemia were not quantified in previous reports, the flow-dependent and -independent pro-ischemic effects of ET-1 have not been sufficiently differentiated. In this study, we applied an NADH fluorescence method to rapidly cross-sectioned frozen heart slices, because NADH is a sensitive marker of ischemia and the distribution of the myocardial ischemic region can be clearly visualized by UV fluorescence. Regional metabolite sampling from frozen heart tissue also reveals the distribution and severity of ischemic myocardium.[13,14] This specially developed sampling method has been shown to be rapid enough to preserve the redox states that existed prior to sectioning, because the sectioning and freezing is performed within 120 milliseconds.[13]

Received for publication April 29, 2005; accepted September 12, 2005.

From the *Cardiopulmonary Division, Department of Internal Medicine, Keio University School of Medicine, Tokyo, Japan; †Department of Emergency and Critical Care Medicine, Keio University School of Medicine, Tokyo, Japan; ‡Department of Biochemistry and Integrative Medical Biology, Keio University School of Medicine, Tokyo, Japan; §National Cardiovascular Center; and ¶Department of Physiology, Tokai University School of Medicine.

Reprints: Shingo Hori, Department of Emergency Medicine, Keio University School of Medicine, 35 Shinanomachi, Shinjuku-ku, Tokyo, 160-8582 Japan (e-mail: shingo@sc.itc.keio.ac.jp).

METHODS

The present investigation conformed with the guidelines for the care and use of laboratory animals published by the US National Institutes of Health (NIH publication No. 85-23, revised 1985).

Animal Preparation

Mongrel dogs weighing 9 to 12 kg (n = 22) were anesthetized with pentobarbital (35 mg/kg iv) and sustained under positive-pressure ventilation. A bilateral thoracotomy was performed at the sixth intercostal space, and the heart was suspended in a pericardial cradle. Heparin was administered intravenously at 500 units/kg. To measure the aortic pressure, a 7F catheter was introduced from the femoral artery into the ascending aorta. A bypass made of silicon tube with metal tip was cannulated from a left subclavian artery to the left anterior descending coronary artery (LAD) on beating heart. The proximal LAD was ligated and cut down to insert a metal tip of the bypass. The diameter of left subclavian artery may not be suitable for coronary diameter but is applicable for bypass-supplier because of avoiding operative failure and excessive bleeding on preparation. A pressure transducer (TP400P, Nihon Koden, Co. Ltd., Tokyo, Japan) and an electromagnetic flow probe (MFV-1200, Nihon Koden, Co. Ltd.) were installed on the bypass circuit, and the coronary perfusion pressure and coronary blood flow were continuously monitored and recorded at thermograph. To record the epicardial electrocardiogram, an electrode made of Ag-AgCl was placed at the center of the perfused area of the left anterior descending coronary artery. To administer the fluorescent dye or non-radioactive microspheres, a 7F catheter was inserted into the left cardiac auricle. The heart rate was fixed at 200 beats per min (bpm) using left atrial pacing. Before starting the experimental protocol, the bypass circuit was occluded for 15 seconds and dogs with reactive hyperemia below 200% of the control flow level were excluded from the study.

Protocol 1: Visualization of Tissue Redox State and Chemical Analysis of Myocardial Ischemia

Fifteen dogs were randomly divided into two groups; eight received the ET-1 administration (endothelin group) and seven underwent coronary stenosis (stenosis group). In the endothelin group, ET-1 (Peptide Institute Inc., Osaka, Japan; 10–150 pmol/min) was administered continuously into the silicon bypass circuit using a micro-infusion pump[15]: this dose reduced the coronary flow by 20% to 40% of the control level. The dosage of ET-1 rapidly increased within 1 minute to get the target flow reduction. The same speed of ET-1 injection could keep in steady state flow reduction, but some dogs with reduced flow level over 40% were excluded from the study. In the stenosis group, coronary inflow was reduced to a comparable level (20%–40% of the control level) by mechanical constriction of the bypass tube. The hemodynamic parameters and epicardial electrocardiogram (ECG) were recorded every minute. The ST segment of the epicardial ECG was measured at 100 milliseconds from the initiation of the QRS complex. At 10 minutes after coronary flow reduction, the beating heart was rapidly cross-sectioned into 4-mm-thick slices along the short-axis plane of the left ventricle using a sampling device specially developed by Hori et al.[13] Within 120 milliseconds after cross-sectioning, a cross-sectional heart slice was compressed to 2.4-mm thickness using precooled aluminum blocks at −190°C. To visualize the tissue redox state of the bypass-perfused areas, from where the cross-sectioned heart slices were obtained, 10 mL of fluorescent dye solution (rhodamine B fluid: 0.1 mg/mL/kg) was injected into the left cardiac auricle 5 seconds before cross-sectioning. The frozen heart slices were fixed in a specially made container filled with precooled freon-12 (CCl_2F_2) and preserved in liquid nitrogen.

Visualization of Tissue Redox State by NADH Fluorescence Imaging

The increase in NADH is the most sensitive and rapid intracellular reaction to occur during ischemia[16,17] and can be visualized as an increase in the NADH fluorescence level in ischemic myocardium. Dual fluorescence photography of NADH (indicating ischemia) and rhodamine B (indicating bypass non-perfused areas) was applied to 15 frozen heart slices. A pair of excitation lights (360 nm, Model B-100A, Ultra-Violet Products, CA) was applied to the frozen heart slices at liquid-nitrogen temperature to visualize the surface NADH and rhodamine B fluorescence in the cross-sectional plane. Two band pass filters were used as secondary filters (Kodak Wratten Gelatin Filter 2E and 47 (Kodak Japan Co. Ltd., Tokyo, Japan) for NADH fluorescence, Kenko Optical Filter YA-3 (Kenko Co. Ltd, Tokyo, Japan) for rhodamine B fluorescence). To quantify the area of myocardial ischemia, the surface NADH fluorescence was analyzed using an image analyzer (IBAS, Carl Zeiss Japan Co. Ltd., Tokyo, Japan) via a CCD video camera (XC-77, Sony Japan Co. Ltd., Tokyo, Japan). A positive NADH-fluorescent area (ischemic area) was defined as an area with a fluorescence intensity two standard deviations above the mean of the simultaneously measured control frozen slice, given another non-ischemic canine cross-sectional heart sample. The bypass-perfused area was defined as the rhodamine B fluorescence-negative area. In a previous study, we observed that rhodamine B, injected into the left cardiac auricle before 5 minutes of cross-sectioning, was not identified in bypass-perfused areas and was clearly present in non-perfused areas.[14] To quantify the amount of ischemic myocardium in the heart slices, the extent of ischemia was expressed as a percentage of the NADH-fluorescent area to the bypass-perfused area in the subendocardial and subepicardial halves of the frozen slices.

To visualize the fluorescent area at a high resolution of up to 10 micrometers, magnified NADH fluorescence photography (×100) was also applied using a dissecting microscope and a Xenon excitation light (Supercure-201S, Fibernics Co. Ltd., Saitama, Japan). To measure the area of microischemia, ischemic foci at the microcirculatory level were selected at random in the endothelin group (1191 counts from 8 randomly selected hearts) and the stenosis group (703 counts from 7 randomly selected hearts). An image analyzer (IBAS, Carl Zeiss Japan Co. Ltd.) was used to measure their short-axis diameters.

Chemical Analysis for Myocardial Metabolites

Cylindrical microsamples weighing about 10 mg (2.4 mm in diameter and 2.4 mm in depth) were drilled in the liquid-nitrogen frozen slices; the microsamples were obtained in perfused area of the subendocardium or subepicardium exhibiting NADH fluorescence. NADH fluorescence was used as a guide to select the sampling sites. Four to six microsamples from each heart slice, for a total of 62 microsamples, were obtained. The NAD, NADH, ATP, creatine phosphate (CP), and lactate concentrations were analyzed in each microsample. NAD and NADH were measured using the bacterial luciferase method,[18] ATP and creatine phosphate were measured using the luciferin-luciferase method,[13] and lactate was measured using the LDH method.[19] The protein content was determined using the Lowry method.[20]

Protocol 2: Systemic and Coronary Hemodynamics

To measure myocardial tissue flow without affecting myocardial ischemia in the same animal, coronary flow was successively reduced in an additional seven dogs, first by stenosis and then by ET-1. After performing a baseline measurement (control group), the bypass was constricted and tissue flow was measured after 10 minutes (stenosis group). The stenosis was then released and once the hyperemia had stabilized, ET-1 (10–150 pmol/min) was administered intracoronary to induce the same degree of hypoperfusion and tissue flow was measured again after 10 minutes (endothelin group). Because of the sustained vasoconstriction induced by ET-1, the order of hypoperfusion induced was fixed, not random.

Myocardial tissue flow was measured using nonradioactive microspheres (15 micrometers in diameter), made of inert plastic labeled with stable heavy elements (Sekisui Plastic Co. Ltd., Tokyo, Japan).[21] Microspheres labeled with barium, iodide, zirconium, or bromine were suspended in 0.1% sodium dodecyl sulfate (SDS) solution, and $0.5–1.0 \times 10^7$ microspheres were infused into the left cardiac auricle. The microspheres were well shaken, and mixed mechanically in a syringe prior to or during the protocol, and no aggregations were observed using light microscopy. Heart tissue samples weighing 3 to 5 g were taken from the subendocardial and subepicardial layers of the bypass-perfused area. Tissues and reference arterial blood samples were dissolved in 1N-KOH, and the microspheres were trapped on filter papers. The samples were irradiated with X-rays, and the X-ray fluorescence activity of each heavy element was measured, the amount of microspheres and the tissue flow in each sample were then calculated.

Statistical Analysis

All values were presented as the means ± SD. Changes in tissue flow and hemodynamic data were determined using a two-way ANOVA. For paired or unpaired data between two groups, Student *t* test was used. *P* values of less than 0.05 were considered statistically significant.

RESULTS

Protocol 1

Hemodynamics and Epicardial Echocardiography

The mean aortic pressures before the experimental protocol were not significantly different between the endothelin group and the stenosis group (Table 1). The hemodynamics did not change significantly throughout the experimental period. The mean doses of endothelin-1 were 46 ± 33 pmol/min. No significant difference in coronary flow reduction was seen in either the endothelin group or the stenosis group. In contrast, the changes in the epicardial ST segment were significantly larger in the endothelin group than in the stenosis group. These results suggest that the myocardial ischemia caused by endothelin-1 differed from that caused by coronary stenosis.

Extension and Distribution of NADH Fluorescence

Figure 1 shows NADH fluorescence photographs of frozen heart slices from both groups. Myocardial ischemia was transmurally distributed in the endothelin group, whereas ischemia distribution was limited to the subendocardium in the stenosis group. Consequently, the total area of myocardial ischemia was larger in the endothelin group than in the stenosis group (Table 2).

Magnified fluorescence photography (×100) was applied to evaluate ischemia formation at the microcirculatory level. Microischemic spots, round or rectangular in shape depending on the direction of the myocardial fibers, were observed in both groups (Fig. 2, upper photographs). To measure the size of the ischemic spots, the short-axis length of the spot was calculated (Fig. 2, lower bar graph). The mean value of the short-axis diameter (less than 120 micrometers) was significantly smaller in the endothelin group than in the stenosis group (61.1 ± 18 versus 76.4 ± 18 micrometers; $P < 0.0001$).

TABLE 1. Changes in ST Segment and Hemodynamics

	Endothelin Group (n = 8) Mean (SD)	Stenosis Group (n = 7) Mean (SD)	Statistics
Changes in ST segment (mV)	6.5 (4.5)	0.7 (0.5)	$P = 0.006$
Coronary blood flow reduction (%)	32.3 (4.5)	34.0 (4.2)	ns
Heart rate (/min)	186 (20)	200 (3.3)	ns
Mean aortic pressure (mm Hg)	99 (8.7)	109 (12)	ns
Mean coronary perfusion pressure (mm Hg)	99 (8.3)	64 (12)	$P < 0.0001$